Compositional Effects on Network Structure of Highly Cross-Linked Copolymers of PEG-Containing Multiacrylates with Acrylic Acid

Robert A. Scott and Nicholas A. Peppas*

School of Chemical Engineering, Purdue University,West Lafayette, Indiana 47907-1283

Received April 20, 1998; Revised Manuscript Received July 19, 1999

ABSTRACT: Novel ionizable polymer networks were prepared from oligo(ethylene glycol) (OEG) multiacrylates and acrylic acid (AA), employing bulk radical photopolymerization techniques. The properties of these materials exhibit a complex dependence on the network structure and composition. Dynamic mechanical analysis and penetrant sorption experiments demonstrated that the cross-linked structure of the materials depends very strongly on the AA content, even in cases where the network chain population is expected to be composed solely of ethylene glycol oligomers. The results indicate that interchain interactions are diminished as the AA content is increased, due to the increased spatial separation of OEG chains. The compositional dependence of the glass transition temperature is qualitatively described by a treatment consistent with that employed for polymer blends, and deviations from ideal blend behavior point to the importance of system-specific free volume changes during the radical polymerization process. Hence, the glass transition temperature and other network properties are closely coupled to the polymerization kinetics.

Introduction

Highly cross-linked polymer glasses formed by the bulk free radical polymerization of multiacrylates and multimethacrylates have been investigated for numerous applications,[1−3] including compact disks, laser video disks, and aspherical lenses. From an applications standpoint, photopolymerization is a particularly attractive technique for preparation of these materials in that it offers a very rapid and highly controllable synthetic route to high strength materials with good optical properties.

Substantial effort has been devoted to developing an understanding of how varying the structure of the multi(meth)acrylate monomer or comonomers and the conditions of photopolymerization impacts the manner in which the cross-linked polymer network is built up over time. Considerable effects, both on the polymerization kinetics and on the final structure of the cross-linked polymer, have been reported.[4−27] Among the very important issues that arise during bulk cross-linking polymerizations of multi(meth)acrylates and that have received considerable attention from investigators are volume relaxation (and the effects of volume relaxation not only on polymer processing and performance but also on the kinetics of the polymerization),[4,11,14,15,18,19] incomplete conversion of monomer and/or double bonds,[4−8,10,12,14] and structural heterogeneity.[5]

Several researchers have reported[4,10,12,14] final double-bond conversions lower than 100% for multi(meth)-acrylate homopolymerizations. Limiting conversions occur due to a dramatically reduced rate of polymerization in the glassy state after vitrification. Kloosterboer[2] reported that the equilibrium degree of conversion can be increased by modifying the monomer structure so as to give a polymer with a lower glass transition temperature, T_g. For example, increasing the length of the spacer between double bonds on a multifunctional monomer was shown[2] to increase the measured equilibrium degree of conversion.

Kloosterboer[4] was also the first to report on the coupling of diffusional and volume relaxation effects on the polymerization kinetics of multi(meth)acrylate monomers. Since the rate of volume relaxation during polymerization lags behind the rate of polymerization, an excess free volume is created. Kloosterboer[4] showed that due to the presence of this excess free volume, increasing the intensity of initiating UV light led to increased double-bond conversions. Essentially, because of the increased radical initiation rate, more double bonds were reacted before the system volume was able to relax to its equilibrium value.

Peppas and co-workers[10,12] examined the effects of varying the cross-linking monomer structure on the photopolymerization behavior of poly(ethylene glycol) dimethacrylates and poly(ethylene glycol) diacrylates. By using di(meth)acrylate monomers having poly(ethylene glycol) (PEG) chains of varying lengths between the double bonds, the researchers were able to systematically control the diffusive and volume relaxation properties of the reacting polymer systems. Hence, the polymerization rate and the measured double-bond conversion increased as the length of the PEG spacer was increased. Both of these trends reflected the increased mobility of the systems having longer PEG chain lengths. Also, methacrylate systems reacted more slowly and exhibited less volume shrinkage than acrylate systems of similar composition.

The cross-linked structure of the polydi(meth)acrylates was probed by swelling and thermomechanical techniques.[9,15] All of the polymers exhibited multiple thermal transitions, with T_g values decreasing with increasing PEG chain length. An approximate treatment of the equilibrium swelling behavior of the polydimethacrylates,[9] based on the Flory−Rehner theory, indicated a highly cross-linked network structure.

Tobita and Hamielec[28,29] developed a pseudokinetic rate constant approach for predicting structural development in radical cross-linking polymerizations. Peppas and co-workers[11,30] also modeled the polymerization behavior of multi(meth)acrylate monomers. Free volume-based models of the polymerization kinetics, inclusive of delayed volume relaxation effects and effects on the

10.1021/ma980612s CCC: $18.00
Published on Web 08/18/1999

initiator efficiency (cage effect), were shown to adequately predict the diffusion-controlled polymerization behavior. Additionally, Monte Carlo simulations (on- and off-lattice)[31−33] provided insight into the heterogeneous evolution of the network structure. Structural heterogeneity was shown to arise due to intrachain cyclization reactions of pendant double bonds on macroradical chains. These cyclization reactions lead to the formation of highly cross-linked and isolated microgel regions early in the polymerization process. These microgel regions then grow together as the polymerization proceeds.

After the investigations of the reaction behavior of poly(ethylene glycol) di(meth)acrylates, the effects of varying the functionality and the chemical composition of the multi(meth)acrylate monomer were further examined by several researchers.[13,14,16−20] The polymerization kinetics, volume shrinkage behavior, and network structure of various di-, tri-, tetra-, and penta-(meth)acrylate polymers were correlated with the monomer structure. Strong mobility-related effects on the rate of polymerization, the measured final double-bond conversions, and the equilibrium volume shrinkage were observed. Additionally, the mechanical properties of the cross-linked polymer glasses were empirically related to the cross-linking density.

Anseth et al.[34] were also able to experimentally quantify the distribution of free volume in polymerizing multi(meth)acrylate systems using mobility-sensitive photochromic probes. This work demonstrated the heterogeneous manner in which the polymer network is assembled, complementing the previous work with stochastic simulations.[31−33]

The present work addresses two significant voids in the existing body of knowledge regarding bulk polymerizations of multi(meth)acrylates. First, in light of the fact that previous efforts to probe the polymer network structure based on mechanical property data have been superficial at best, the network structure of model multiacrylate systems has been exhaustively examined as a function of various compositional variables. Specifically, the network structure has been carefully treated in the context of competing contributions to the bulk behavior from backbone chains, built up by radical polymerization, and "cross-linking" chains, supplied by the multi(meth)acrylate monomer. Second, the effects of copolymerization with a monovinyl comonomer have been investigated. The present work represents the first fundamental study of the properties of highly cross-linked acrylate copolymers.

The model multiacrylate networks investigated were derived from the acrylate di- and triesters of various oligo(ethylene glycols) and from acrylic acid (AA). The study of these materials offered the opportunity to explore the use of copolymerization techniques as a route to "tunable" and functionalized polymers, with properties tailored to the demands of various applications. By precisely controlling the ethylene glycol and AA contents, polymer behavior and properties, including hydrophilicity, pH sensitivity, and complexation, were manipulated.

Experimental Section

Materials. The various monomers used are shown in Figure 1. The diacrylates were ethylene glycol diacrylate (EGDA, $n = 1$), di(ethylene glycol) diacrylate (DEGDA, $n = 2$), tri(ethylene glycol) diacrylate (TrEGDA, $n = 3$), poly(ethylene glycol) (MW = 200) diacrylate (PEG200DA, $n \approx 4$), and poly(ethylene glycol) (MW = 400) diacrylate (PEG400DA, $n \approx 9$) (Polysciences, Warrington, PA). The triacrylates were trimethylolpropane triacrylate (TrMPTrA, Polysciences) and a series of ethoxylated analogues (Aldrich, Milwaukee, WI) of TrMPTrA. The analogues contained 3 (PEG170TrA), 7 (PEG290TrA), and 14 (PEG500TrA) ethoxy groups per monomeric unit. The AA molar feed content in multiacrylate copolymers was varied from 0 to 40 mol %, based on double bonds. The multiacrylate monomers were used as received, without further purification.

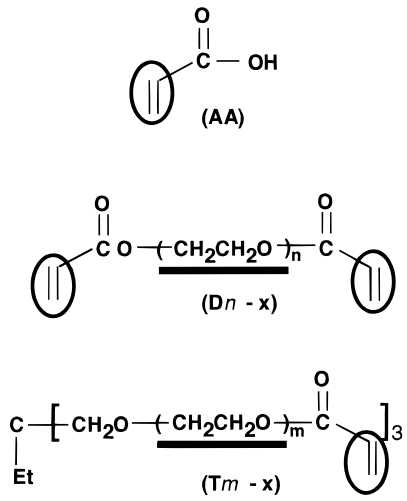

Figure 1. Structures of the various monomers used in the preparation of multiacrylate homo- and copolymers.

Methods. Monomer mixtures were prepared by mixing distilled AA (Aldrich) and a multiacrylate monomer in appropriate quantities. A typical formulation contained 40 mol % AA and 60 mol % PEG200DA, with photoinitiator 2,2-dimethoxy-2-phenylacetophenone (DMPA, Aldrich) added at a concentration of 1 wt %, based on total monomer weight. Thin polymer films were prepared by reacting monomer solutions confined between glass plates separated by Teflon spacers of approximate thickness 0.8 mm. Polymerizations were carried out in a N_2 atmosphere and were initiated by ~1 mW/cm^2 of UV light from a mercury arc lamp (Ultracure 100, EFOS, Mississaugua, Ontario, Canada). The exposure time was 25 min. To ensure that all samples had the same thermal history, polymer films were heated to 60 °C in a vacuum oven for ~12 h immediately following polymerization.

Glass transition temperature, T_g, values for polymer films were determined by dynamic mechanical analysis (DMA). DMA experiments were performed in the resonant frequency mode with an oscillation amplitude of 0.20 mm on a dynamic mechanical analyzer (model DMA 983, TA Instruments, New Castle, DE). Sample lengths were adjusted to give an average resonant frequency of 5.5 ± 0.3 Hz, and T_g was measured as the maximum in the damping factor, tan δ, observed at the resonance frequency during temperature scans performed at a rate of 10 °C/min.

The swelling behavior of polymer films was examined by immersing dry polymer slabs (approximate dimensions: 13 mm × 13 mm × 0.8 mm) of known weight in acetone, a solvent of high thermodynamic compatibility for the multiacrylate homo- and copolymers, or in aqueous buffer having pH 2.2 (HCl buffer) or pH 7.4 (phosphate buffer). Samples were kept at 30 °C in a thermostated water bath, and the slabs were periodically removed and weighed in order to determine the rate of penetrant uptake. Gravimetric measurements were performed until the change in the swollen polymer weight was less than 0.0001 g over a 24 h period, at which point the polymers were assumed to be at equilibrium.

Results and Discussion

Molecular Design. The structures of the various monomers used in the preparation of polymer networks

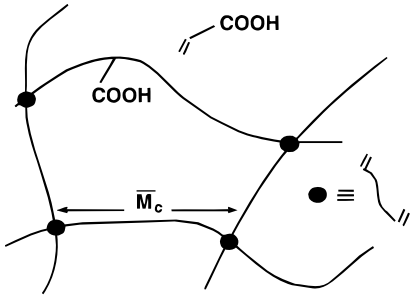

Figure 2. Depiction of network structure for loosely cross-linked poly(acrylic acid).

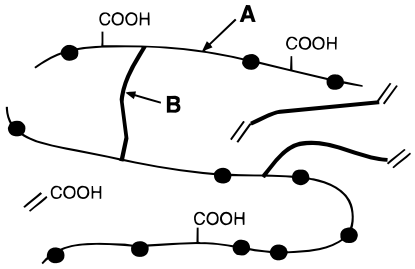

Figure 3. Network structure of the poly(multiacrylate-*co*-AA) system.

are shown in Figure 1. Each polymer network was prepared in bulk from a mixture of one di- or triacrylate with a quantity of AA varying from 0 to 40 mol %, based on double bonds. This experimental approach provided networks with a spectrum of PEG and AA contents and facilitated examining the independent effects on the network structure of varying the PEG chain length or of varying the AA content.

Figures 2 and 3 demonstrate the manner in which the network morphology changes at the molecular level as the AA content or the PEG chain length is varied. Here, we consider a network formed from AA and an oligo(ethylene glycol) diacrylate. In loosely cross-linked systems (those with high AA content), each diacrylate unit forms a tetrafunctional cross-link, and each pair of cross-links is separated by a poly(acrylic acid) (PAA) chain (Figure 2). The population of network chains is composed solely of PAA chains, and the effect of the tie point structure on the polymer network properties is minimal.

We have been interested, however, in materials having relatively low AA contents, and Figure 3 illustrates that the situation is very different for such systems. As the cross-link concentration (relative concentration of diacrylate monomer) is increased, the PAA chains between cross-linking sites become increasingly short, until at sufficiently high cross-linking densities the PAA chains are of a length comparable to that of the PEG chains contributed by the cross-linking monomer. Clearly then, when the AA content is low in copolymerizations of AA with PEG-containing multiacrylates, two types of network chains may influence the observed macroscopic polymer properties. The first type of network chain is the poly(acrylate-*co*-acrylic acid) chain that is built up as the polymerization proceeds by radical propagation through acrylate and AA double bonds. This chain is marked as chain A in Figure 3. The second type of network chain is the PEG chain which connects acrylate functionalities within each macromer unit (chain B).

Taking advantage of an experimental design that facilitates independent control of the AA content and of the PEG chain length, the goals of the present work are to examine how each type of network chain contributes to the bulk behavior of the polymer network and to demonstrate the extent to which each type of network chain represents an independently "tunable" parameter in the development of materials with precisely controlled properties.

Table 1. Compositions of the Various Diacrylate Systems Examined[a]

PEG units	M_c (g/mol)	system	w_{AA}	f_{AA}	PEG/AA (mer/mer)
1 (EGDA)	170	D1	0	0	0.50
		D1−3	0.0255	0.0300	0.49
		D1−10	0.0866	0.101	0.45
		D1−11	0.0964	0.112	0.44
		D1−40	0.360	0.399	0.30
2 (DEGDA)	214	D2	0	0	1.0
		D2−3	0.0298	0.0436	0.96
		D2−10	0.0741	0.106	0.89
		D2−20	0.144	0.200	0.80
		D2−40	0.311	0.401	0.60
3 (TrEGDA)	258	D3	0	0	1.5
		D3−3	0.0170	0.0300	1.5
		D3−10	0.0585	0.100	1.4
		D3−27	0.173	0.272	1.1
		D3−40	0.271	0.400	0.9
∼4 (PEG200DA)	326	D4	0	0	2.0
		D4−3	0.0156	0.0322	1.9
		D4−10	0.0512	0.102	1.8
		D4−34	0.183	0.337	1.3
		D4−40	0.241	0.409	1.2
∼9 (PEG400DA)	526	D9	0	0	4.5
		D9−3	0.0126	0.0446	4.3
		D9−10	0.0293	0.0992	4.1
		D9−53	0.236	0.530	2.1
		D9−40	0.155	0.400	2.7

[a] The parameters w_{AA} and f_{AA} are the weight fraction and mole fraction (based on double bonds), respectively, of AA in comonomer mixtures. Here, M_c values are the molecular weights of the diacrylate monomers.

Table 2. Compositions of the Various Triacrylate Systems Examined[a]

PEG units	M_c (g/mol)	system	w_{AA}	f_{AA}	PEG/AA (mer/mer)
∼3 (PEG170TrA)	299	T3	0	0	1.0
		T3−3	0.0165	0.0321	0.97
		T3−10	0.0500	0.0943	0.91
		T3−40	0.259	0.409	0.59
∼6 (PEG290TrA)	416	T6	0	0	2.3
		T6−3	0.0111	0.0310	2.2
		T6−10	0.0378	0.0990	2.1
		T6−40	0.189	0.394	1.4
∼10 (PEG500TrA)	622	T10	0	0	4.6
		T10−3	0.0111	0.0450	4.5
		T10−10	0.0248	0.0968	4.2
		T10−40	0.135	0.397	2.8

[a] The parameters w_{AA} and f_{AA} are the weight fraction and mole fraction (based on double bonds), respectively, of AA in comonomer mixtures.

Tables 1 and 2 list the various compositions prepared, using diacrylate and triacrylate monomers, respectively. Provided in the tables are the multiacrylate monomer names, the theoretical value of the molecular weight between cross-links, M_c, for polymers prepared by homo- or copolymerization from each multiacrylate monomer, the weight and mole fractions of added AA, and the ratio of PEG units to poly(acrylate-*co*-AA) units in the prepared polymer networks. A code name beginning with D (for diacrylates) or T (for triacrylates) was used to uniquely identify each copolymer according to PEG chain length and AA content. The theoretical value of

M_c for diacrylate systems is the molecular weight of the diacrylate monomer. The theoretical value of M_c for triacrylate systems is the molecular weight of the linear PEG-based chain connecting and comprising any two of the three double bonds on the triacrylate monomer. The molecular weight of the PEG-based branch leading to the third double bond is accounted for separately, as a portion of an additionally contributed network chain. Theoretical M_c values calculated in this manner are approximate values which capture the primary compositional dependence of the network structure. The accuracy of the M_c approximation depends on the extent of chain cyclization, the degree of conversion, and the AA content. The tables clearly show that a wide range of compositions was considered.

Structural Analysis Using Copolymerization Equation. To obtain structural information for the PEG−AA copolymer systems, reactivity ratios r_1 (for AA) and r_2 (for multiacrylate double bonds) were calculated on the basis of the Alfrey−Price $Q-e$ scheme.[35] The following Q and e values[36] were used for AA (monomer 1) and for the multiacrylates (monomer 2): $Q_1 = 0.83$, $e_1 = 0.88$, $Q_2 = 0.48$, $e_2 = 1.28$. Q_2 and e_2 were approximated using values tabulated for glycidyl acrylate, an acrylate monomer having a structure similar to that of the PEG-containing multiacrylates. Calculated values of r_1 and r_2 were $r_1 = 2.46$ and $r_2 = 0.35$. Free and pendant double bonds were assumed to have equal reactivity. The accuracy of this assumption degrades at extremely low and extremely high levels of conversion.[3]

Using the calculated reactivity ratio values, the number-average sequence lengths, n_1 and n_2, and the comonomer feed compositions, f_1 and f_2, were calculated as a function of double-bond conversion, p, for AA−multiacrylate mixtures having various initial AA feed compositions, f_{1o}. The terms n_1 and n_2 represent the average number of AA and acrylate units, respectively, which appear in uninterrupted sequences in the polymer network.[35] Calculated results are shown in Figure 4 for systems with $f_{1o} = 0.03$, $f_{1o} = 0.10$, and $f_{1o} = 0.40$. The trends in the conversion dependence of f_1 and f_2 for all cases reflect the fact that r_1 is greater than r_2, leading to an increased rate of incorporation of AA, relative to that of the multiacrylate monomer.

Clearly, for relatively low AA concentrations the structure of the network backbone approximates that of a polyacrylate homopolymer. In this case, almost all sites along the network backbone are linked to other backbone sites by PEG chains. Thus, the PEG chains are expected to be in extremely close proximity. However, copolymers containing 40% AA have a backbone structure characterized by alternating groups of AA and PEG units. These individual groups have lengths on the order of 2−3 monomer units, and the PEG chains between backbone sites are therefore more widely separated than at lower AA concentrations. On the basis of these considerations, substantial compositional effects on the copolymer properties are expected.

The calculated data presented in Figure 4 accurately describe the limiting case of a kinetically controlled free radical polymerization mechanism. However, it is not unreasonable to expect that diffusional considerations will lead to values of r_1 and r_2 that vary from those calculated according to the $Q-e$ scheme. Thus, on the basis of relative monomer size considerations, it can be assumed that when the propagation reaction is diffusion-controlled, r_1 increases and r_2 decreases. As a result, the calculated low-conversion values of n_1 and n_2 should be viewed as lower and upper limits, respectively. Figure 4 demonstrates that the molecular-level structure of the copolymer network depends very strongly on the AA content for any given multiacrylate monomer.

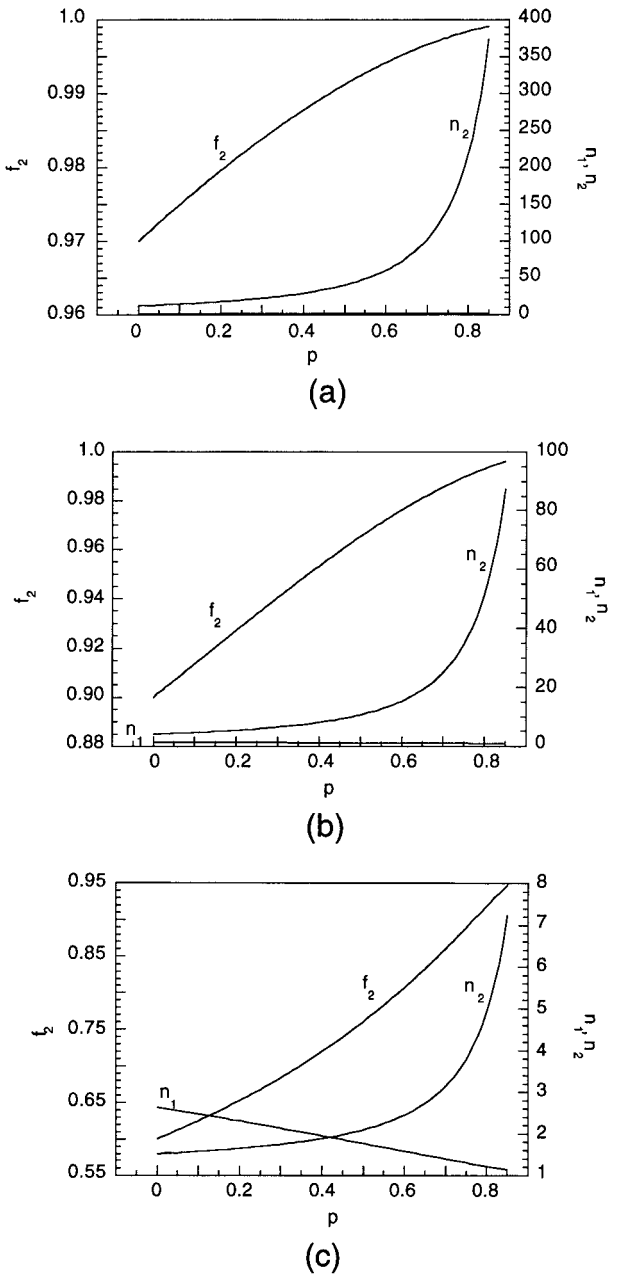

Figure 4. Calculated conversion dependence of the number-average sequence length, n_1, of AA, the number-average sequence length, n_2, of the multiacrylate monomer, and the fractional concentration of the multiacrylate monomer in the feed, f_2. The initial values of f_2 were 0.97 (a), 0.90 (b), and 0.60 (c).

Compositional Effects on Viscoelastic Behavior. To experimentally probe the structural changes that accompanied variations in the AA content or in the length of the PEG chain contributed by the multiacrylate monomer, the copolymers' dynamic mechanical behavior was considered. Using a dynamic mechanical analyzer, the temperature dependencies of the shear storage modulus, G', and the shear loss modulus, G'', were measured for samples of various compositions.

Table 3. Measured Glass Transition Temperatures T_g for Poly(diacrylate) Homo- and Copolymers

PEG units	M_c (g/mol)	system	T_g (±5 °C)	$T_{g\infty}$ (°C)
1	170	D1	61	45
		D1−3	73	47
		D1−10	90	51
		D1−11	116	51
		D1−40	150	67
2	214	D2	118	24
		D2−3	111	26
		D2−10	115	30
		D2−20	117	36
		D2−40	115	49
3	258	D3	65	9
		D3−3	73	11
		D3−10	76	15
		D3−27	79	26
		D3−40	79	36
∼4	326	D4	47	−5
		D4−3	50	−3
		D4−10	53	1
		D4−34	59	15
		D4−40	68	22
∼9	526	D9	−12	−26
		D9−3	−11	−24
		D9−10	−7	−22
		D9−53	29	5
		D9−40	12	−5

Table 4. Measured Glass Transition Temperatures T_g for Poly(triacrylate) Homo- and Copolymers

PEG units	M_c (g/mol)	system	T_g (±5 °C)	$T_{g\infty}$ (°C)
∼3	299	T3	108	3
		T3−3	113	5
		T3−10	111	8
		T3−40	131	30
∼6	416	T6	39	−15
		T6−3	40	−14
		T6−10	42	−11
		T6−40	59	7
∼10	622	T10	−8	−31
		T10−3	−8	−29
		T10−10	−4	−27
		T10−40	18	−12

Two types of analyses were performed using the measured dynamic mechanical data. First of all, the glass transition temperature, T_g, was measured for each sample as the temperature at which the maximum in tan δ was observed. The measured T_g values were then correlated with the known copolymer composition in order to provide an indication of the manner in which the structure varied with composition. Second, the equilibrium or rubbery plateau value of the shear storage modulus, G'_e, was measured for each sample and treated using rubber elasticity theory. This analysis provided additional insight into the relationship between composition and the network structure.

Tables 3 and 4 list the measured glass transition temperatures for the various copolymer networks. Table 3 contains data for the diacrylate networks, whereas Table 4 contains data for the triacrylate networks. Clearly, T_g is a decreasing function of the PEG chain length for both types of networks (diacrylates and triacrylates). These results reflect the decreasing dependence of the cross-linking density and the increasing dependence of the PEG content on the PEG chain length, at any given molar concentration of AA. Also, the tables show that a wide range of T_g values was accessible by varying the compositional parameters of the networks.

Anomalous behavior was observed for the D1-*x* systems. The surprisingly low values of T_g for the D1-*x* systems were a reflection of the very low degrees of conversion obtained during polymerization of the D1 monomer, in the presence or in the absence of added AA. Typically, the polymerization stopped when only 30%−40% of the available double bonds had reacted, as measured by differential scanning photocalorimetry. Conversions of at least 65% were obtained for all other systems. Thus, incomplete network formation, due to mobility considerations over the course of the polymerization, led to diminished T_g values for the D1-*x* systems.

Tables 3 and 4 also reveal that T_g increased with increasing AA content for all but the most highly cross-linked systems. This trend reflects a copolymer effect arising due to the increased contribution of PAA segments to the bulk properties of the poly(acrylate-*co*-AA) backbone.

Clearly, the observed trends in T_g suggest competing effects of cross-linking and copolymerization as the PEG chain length and the AA content were varied. Thus, an analysis based on the free volume effects of cross-linking was performed in order to try to capture these effects in a molecular framework.

The following expression represents the Fox and Loshaek[37] description of cross-linking effects on the glass transition, wherein the difference, $T_{g\infty} - T_g$, of the observed glass transition temperature for a cross-linked polymer, T_g, and that which would be observed if all cross-links in the system were severed, $T_{g\infty}$, was related to the change in free volume due to cross-linking. The proportionality constant for this relationship was α_f, the difference of the polymer thermal expansion coefficients in the rubbery and glassy states, α_l and α_g, respectively:[37]

$$-\frac{2\rho N_A}{f M_c}\theta_1 = \alpha_f(T_{g\infty} - T_g) \qquad (1)$$

Here, ρ is the polymer density, f is the cross-link functionality, and N_A is Avogadro's number. The parameter θ_1 is the reduction in free volume per cross-link, while the quotient which precedes θ_1 is the number concentration of cross-links in the system.

An analysis of this type for the PEG−AA copolymer systems requires an accurate estimate of $T_{g\infty}$. $T_{g\infty}$ is easily calculated or measured for loosely cross-linked systems, in which the network chains are well-defined. The calculation of $T_{g\infty}$ for the multiacrylate homo- and copolymers, however, is significantly more complicated. Our calculation of $T_{g\infty}$ was based on the fact that the polymer networks prepared by radical copolymerization of AA and various multiacrylates are identical in chemical structure to hypothetical condensation networks formed by the esterification of PAA with PEG. Thus, $T_{g\infty}$ values were calculated by hypothetically deconstructing the copolymer networks to give blends of PEG and PAA. Appropriate $T_{g\infty}$ values were then calculated utilizing the following equation, which relates the T_g of an ideal blend (here, $T_{g\infty}$) to the T_g values of the constituent linear polymers:[38]

$$T_{g\infty} = w_{AA}T_{g,AA} + w_{PEG}T_{g,PEG} \qquad (2)$$

Here, w_{AA} and w_{PEG} are the weight fractions of PAA and PEG, respectively, in the blend obtained upon deconstruction of the network. These values were easily calculated on the basis of the multiacrylate and AA feed

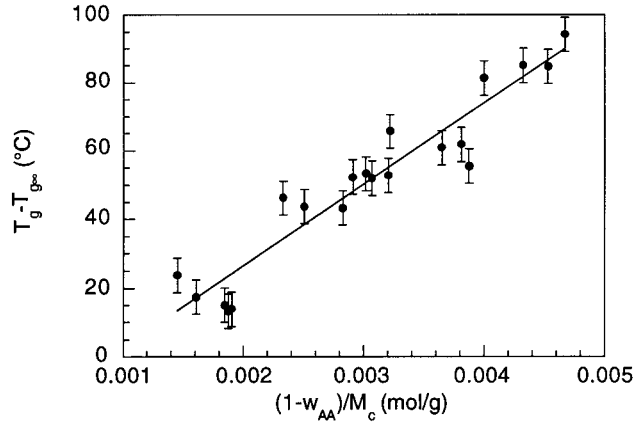

Figure 5. Compositional dependence for diacrylate copolymer systems of the deviation, $T_g - T_{g\infty}$, of the experimental glass transition temperature, T_g, from the theoretical value, $T_{g\infty}$, calculated based on a blend of linear PEG and PAA chains.

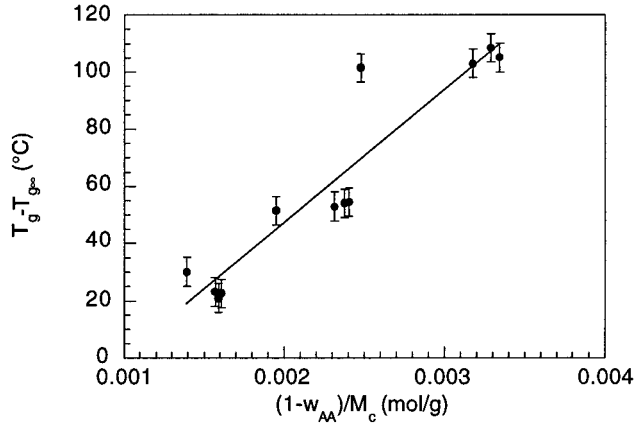

Figure 6. Compositional dependence for triacrylate copolymer systems of the deviation, $T_g - T_{g\infty}$, of the experimental glass transition temperature, T_g, from the theoretical value, $T_{g\infty}$, calculated based on a blend of linear PEG and PAA chains.

concentrations. The T_g values for linear PAA and linear PEG were $T_{g,AA} = 379$ K and $T_{g,PEG} = 213$ K.

Tables 3 and 4 provide calculated values of $T_{g\infty}$ for various compositions. Clearly, the largest deviations from ideal blend behavior were observed for the most highly cross-linked polymer networks. As M_c increased, T_g was more accurately described by the ideal blend treatment.

Figures 5 and 6 demonstrate that the independent effects on T_g of varying the AA content and the PEG chain length in multiacrylate copolymer systems may be reasonably described by a free volume-based dependence of $T_g - T_{g\infty}$ on $(1 - w_{AA})/M_c$. The slope which describes the dependence for the triacrylate systems is twice that which describes the dependence for the diacrylate systems. This difference of slopes is due to the functionality dependence of the cross-link concentration.

Clearly, the measured dependence of T_g on the copolymer composition reflected a strong compositional dependence of the network structure. Compositional effects on the network structure were further probed using rubber elasticity theory. The general Flory equation describes the dependence of the rubbery polymer shear modulus on the concentration of network chains in the system:

$$G'_e = A_\phi \nu_e RT \tag{3}$$

Table 5. Measured and Calculated Structural Parameters for Diacrylate Systems Having Various AA Contents[a]

PEG units	M_c (g/mol)	system	log G'_e (±0.1 Pa)	$A_\phi \nu_e \times 10^3$ (mol/mL)	A_ϕ
1	170	D1	8.7	140	19
		D1−3	8.7	140	19
		D1−10	8.7	150	22
		D1−40	8.7	140	30
2	214	D2	7.9	18	3.1
		D2−3	7.9	19	3.4
		D2−10	7.8	18	3.3
		D2−20	7.7	13	2.5
		D2−40	7.4	7.0	1.7
3	258	D3	7.7	15	3.0
		D3−3	7.6	14	2.8
		D3−10	7.6	13	2.9
		D3−27	7.3	5.7	1.4
		D3−40	7.3	5.7	1.6
∼4	326	D4	7.6	12	3.1
		D4−3	7.6	12	3.0
		D4−10	7.5	11	2.9
		D4−34	7.1	3.9	1.2
		D4−40	7.1	4.0	1.3
∼9	526	D9	7.2	5.9	2.5
		D9−3	7.2	5.7	2.4
		D9−10	7.1	5.5	2.4
		D9−53	7.0	3.2	1.7
		D9−40	7.0	3.5	1.7

[a] The parameter G'_e is the shear storage modulus measured at the rubbery plateau, A_ϕ is the structural factor, and ν_e is the network chain concentration.

Here, G'_e is the equilibrium or rubbery plateau value of the shear storage modulus, A_ϕ is the structural factor, ν_e is the concentration of network chains (moles/volume), R is the universal gas constant, and T is the absolute temperature.

The term ν_e is related to M_c and the AA content:

$$\nu_e = \frac{\rho(1 - w_{AA})}{M_c} \tag{4}$$

The term A_ϕ accounts for deviations from ideal rubber elastic behavior:

$$A_\phi = \frac{\bar{r}_o^{\,2}}{\bar{r}_f^{\,2}}\left(1 - 2\frac{M_c}{M_n}\right) \tag{5}$$

The first term on the right-hand side of eq 5 is the front factor, which is equal to one in the limit of a perfectly affine network or one in which there is no cross-link motion. Phantom networks, or those in which there is some cross-link mobility, typically have front factor values less than one. The second term on the right-hand side of eq 5 is a reduction factor which accounts for the fact that, due to the presence of dangling chain ends, not all chains are elastically active.

Tables 5 and 6 show the measured values of G'_e, as a function of the AA content and of the PEG chain length. Clearly, increasing the AA content and increasing the PEG chain length led to reduced values of G'_e. The dependence on the number of ethylene glycol units per multiacrylate monomer is expected, on the basis of the cross-linking density dependence of G'_e, described by eqs 3 and 4. A careful consideration of the measured dependence of G'_e on the AA content, however, offers valuable insight into the molecular-level effects of multiacrylate copolymerization with AA.

Using the theoretical values of M_c and the known values of the polymer density and the temperature at

Table 6. Measured and Calculated Structural Parameters for Triacrylate Systems Having Various AA Contents[a]

PEG units	M_c (g/mol)	system	log G'_e (±0.1 Pa)	$A_\phi \nu_e \times 10^3$ (mol/mL)	A_ϕ
~3	299	T3	8.2	47	5.5
		T3−3	8.2	39	4.7
		T3−10	8.0	27	3.4
		T3−40	7.7	13	2.0
~6	416	T4	7.6	14	2.4
		T4−3	7.6	13	2.3
		T4−10	7.6	13	2.2
		T4−40	7.3	6.6	1.4
~10	622	T10	7.3	7.2	1.8
		T10−3	7.3	6.9	1.8
		T10−10	7.3	7.3	1.9
		T10−40	7.1	4.2	1.2

[a] The parameter G'_e is the shear storage modulus measured at the rubbery plateau, A_ϕ is the front factor, and ν_e is the network chain concentration.

the rubbery plateau, A_ϕ values were calculated from the experimental modulus data for each copolymer composition using eqs 3 and 4. The results of the calculations are given in Tables 5 and 6. The tables show several important trends. First of all, all calculated A_ϕ values were greater than one. This finding suggests that the network chains are highly entangled, leading to decreased chain flexibility and mobility and the formation of effective cross-links. Second, the A_ϕ values showed a very strong decreasing dependence on the AA content. The effect of copolymerization with increasing quantities of AA, as demonstrated by structural analysis based on the monomer reactivity ratios, is to more frequently interrupt continuous poly(multiacrylate) sequences along the network backbone. Higher AA contents and increased separation of PEG-containing units will lead to a decrease in the number of entangled chains. This decrease in entanglements was monitored by the parameter A_ϕ. Last, A_ϕ decreased as the PEG chain length was increased, reflecting a free volume-based decrease in the number of entanglements.

Compositional Effects on Equilibrium Swelling Behavior. The molecular structure of the poly(multiacrylate-*co*-AA) systems was further probed by examining their equilibrium swelling behavior. Values of the equilibrium weight swelling ratio were measured gravimetrically in various swelling media. Compositional effects on the swelling behavior were isolated from ionization effects by studying the swelling behavior in acetone, a penetrant of high thermodynamic compatibility for the copolymer networks. By then investigating the swelling behavior in aqueous buffers having pH 2.2 and pH 7.4, the effects of the degree of ionization and the ratio of PEG and AA mers on the strength of polymer−water interactions were determined.

Figure 7 shows a typical plot of the polymer weight swelling ratio, q, as a function of time over the course of a swelling experiment in acetone. Tables 7 and 8 show the equilibrium weight swelling ratio, q_∞, for various di- and triacrylate copolymer systems in acetone. Also shown in the table are values of the polymer solubility parameter, δ_2, calculated based on group contribution methods.[39] Comparison of the calculated δ_2 values with the solubility parameter, δ_1, of the penetrant, in this case acetone, provides an indication of polymer−penetrant compatibility. Values for δ_1 and δ_2 which differ by less than 1 (cal cm^{-3})$^{1/2}$ indicate a highly compatible polymer−penetrant system. The solubility parameter δ_2 for acetone is equal to 9.9 (cal cm^{-3})$^{1/2}$.

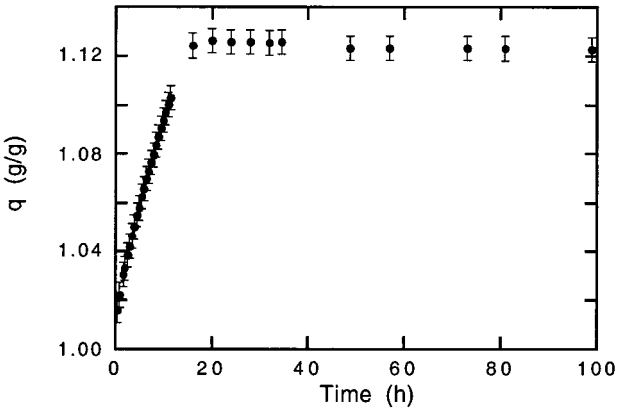

Figure 7. Representative plot of the time dependence of the polymer weight swelling ratio, q, over the course of a dynamic swelling experiment in acetone at 30 °C.

Table 7. Measured Swelling Parameters and Calculated Solubility Parameters for Diacrylate Systems in Acetone Having Various AA Contents[a]

M_c (g/mol)	system	PEG/AA (mer/mer)	q_∞ (g/g)	δ_2 (cal cm^{-3})$^{1/2}$
214	D2	1.0	1.105	9.9
	D2−3	0.96	1.117	9.9
	D2−10	0.89	1.126	9.9
	D2−20	0.80	1.131	10
	D2−40	0.60	1.162	10
258	D3	1.5	1.112	9.8
	D3−3	1.5	1.114	9.8
	D3−10	1.4	1.125	9.9
	D3−27	1.1	1.145	10
	D3−40	0.9	1.165	10
326	D4	2.0	1.116	9.8
	D4−3	1.9	1.119	9.8
	D4−10	1.8	1.127	9.8
	D4−34	1.3	1.143	9.9
	D4−40	1.2	1.172	10

[a] The parameter M_c is the theoretical value of the molecular weight between cross-links, q_∞ is the equilibrium value of the weight swelling ratio, and δ_2 is the polymer solubility parameter, calculated based on group contribution methods.[39]

Table 8. Measured Swelling Parameters and Calculated Solubility Parameters for Triacrylate Systems in Acetone Having Various AA Contents[a]

M_c (g/mol)	system	PEG/AA (mer/mer)	q_∞ (g/g)	δ_2 (cal cm^{-3})$^{1/2}$
299	T3	1.0	1.091	9.5
	T3−3	0.97	1.094	9.6
	T3−10	0.91	1.105	9.6
	T3−40	0.59	1.162	9.8
416	T6	2.3	1.121	9.6
	T6−3	2.2	1.125	9.6
	T6−10	2.1	1.130	9.6
	T6−40	1.4	1.171	9.8
622	T10	4.6	1.181	9.6
	T10−3	4.5	1.186	9.6
	T10−10	4.2	1.188	9.6
	T10−40	2.8	1.222	9.7

[a] The parameter M_c is the theoretical value of the molecular weight between cross-links, q_∞ is the equilibrium value of the weight swelling ratio, and δ_2 is the polymer solubility parameter, calculated based on group contribution methods.[39]

The data in Tables 7 and 8 show an increasing dependence of q_∞ on the AA content for each di- and triacrylate system, with negligible effects observed as the PEG chain length was varied. On the basis of the calculated δ_2 values, which are all very close to δ_1, the observed behavior was not due to composition-dependent changes in polymer−solvent compatibility. In fact,

Table 9. Measured Swelling Parameters and Calculated Solubility Parameters for Diacrylate Systems at pH 2.2 and at pH 7.4, Having Various AA Contents[a]

M_c (g/mol)	system	PEG/AA (mer/mer)	q_∞ (g/g) pH 2.2	q_∞ (g/g) pH 7.4	δ_2 (cal cm^{-3})$^{1/2}$
170	D1	0.50	1.023	1.024	10
	D1−40	0.30	1.136	1.184	10
214	D2	1.0	1.052	1.051	9.9
	D2−40	0.60	1.145	1.494	10
258	D3	1.5	1.071	1.071	9.8
	D3−40	0.9	1.171	1.471	10
326	D4	2.0	1.092	1.102	9.8
	D4−3	1.9	1.123	1.119	9.8
	D4−10	1.8	1.133	1.151	9.8
	D4−40	1.2	1.160	1.468	10
526	D9	4.5	1.320	1.315	9.7
	D9−40	2.7	1.347	1.643	9.8

[a] The parameter M_c is the theoretical value of the molecular weight between cross-links, q_∞ is the equilibrium value of the weight swelling ratio, and δ_2 is the polymer solubility parameter, calculated based on group contribution methods.[39]

in the case of the diacrylate systems, copolymerization with increasing quantities of AA led to increased equilibrium swelling even while driving δ_2 away from the δ_1 value of 9.9 (cal cm^{-3})$^{1/2}$. Clearly then, the observed dependence of q_∞ on the AA content was due to a structure-based change in the ability of the network to accommodate the diffusing penetrant. Incorporation of AA along the network backbone led to a looser equilibrium mesh by reducing PEG−PEG entanglements. This effect of AA content on entanglements and interchain interactions was also reflected in the structural factor, A_ϕ, calculated as described in the preceding section by rubber elasticity analysis of the DMA data.

Table 9 shows the equilibrium swelling data measured at pH 2.2 and at pH 7.4 for various diacrylate copolymers. The solubility parameter for water is 23.4 (cal/cm^3)$^{1/2}$. In comparing Tables 7 and 9, which contain the equilibrium swelling data for the diacrylate copolymer systems in acetone and in the two aqueous buffers, several trends are observed. First, the qualitative effects of varying the AA content were independent of the swelling agent. In all cases, higher equilibrium degrees of swelling were observed as the AA content was increased. However, the data collected for AA-containing systems in aqueous buffer indicated a strong pH sensitivity of q_∞. The AA copolymers exhibited substantially higher q_∞ values at pH 7.4, above the PAA pK_a of $\sim$ 5, than at pH 2.2. These higher q_∞ values reflect the effects of chain ionization on the swelling behavior. The equilibrium swelling behavior of the multiacrylate homopolymers did not vary with pH.

Tables 7 and 9 also reveal that the effects of varying the PEG chain length were dependent on the nature of the swelling agent. Table 7 shows that as the PEG chain length was varied over the range of 2−4 ethylene glycol units, there were negligible effects on q_∞ at any given AA content. However, in pH 2.2 buffer (Table 9), q_∞ was a monotonically increasing function of the PEG chain length. This difference in measured behavior for the two swelling agents suggested that the effects observed at pH 2.2 were indicative of changes in the nature of polymer−solvent interactions as the composition was varied, rather than of network structural effects.

This hypothesis was examined using an analysis based on a modified version of the Flory−Rehner description of the equilibrium swelling of polymer gels cross-linked in the solid state.[40] This modified description of the equilibrium swelling behavior includes the effects of a non-Gaussian chain length distribution (appropriate for the highly cross-linked PEG−AA networks), chain ionization, and composition-dependent structural factor A_ϕ:[40−43]

$$\frac{1}{M_c} = \frac{2}{M_n} - \frac{(\bar{v}/V_1)[\ln(1 - v_{2,s}) + v_{2,s} + \chi v_{2,s}^2]\left[1 - \frac{1}{N}v_{2,s}^{2/3}\right]^3}{A_\phi\left[v_{2,s}^{1/3} - \frac{v_{2,s}}{2}\right]\left[1 + \frac{1}{N}v_{2,s}^{1/3}\right]^2} + \frac{\frac{\rho}{4I}\left[\frac{v_{2,s}}{M_r}\right]^2\left[\frac{K_a}{10^{-pH} + K_a}\right]^2\left[1 - \frac{1}{N}v_{2,s}^{2/3}\right]^3}{A_\phi\left[v_{2,s}^{1/3} - \frac{v_{2,s}}{2}\right]\left[1 + \frac{1}{N}v_{2,s}^{1/3}\right]^2} \quad (6)$$

The parameter M_c is the theoretical value of the molecular weight between cross-links, $\bar{v}$ is the specific volume of the polymer, V_1 is the molar volume of the penetrant, M_n is the number-average molecular weight of the linear chains in the absence of cross-links ($\approx$75 000 for multiacrylate polymer systems), $v_{2,s}$ is the polymer volume fraction in the swollen state, and χ is the Flory polymer−solvent interaction parameter. The term which appears on the right-hand side of eq 6 and contains the pH of the swelling agent and the dissociation constant, K_a, of the polyacid accounts for the ionic contribution to swelling. The parameter I is the ionic strength of the swelling agent. The factors containing $1/N$ which appear in the last two terms on the right-hand side of eq 6 account for the non-Gaussian chain length distribution. The parameter N is the number of links per network chain and is defined as follows:

$$N = \frac{\lambda M_c}{M_r} \quad (7)$$

The parameter λ is the number of links per repeating unit (3 for PEG), and M_r is the molecular weight of a repeating unit (44.05 g/mol for PEG).

Thus, with $v_{2,s}$ values calculated from the equilibrium swelling data, the only unknown parameter in eq 6 was the Flory polymer−solvent interaction parameter, χ. By substituting the composition-dependent values of $v_{2,s}$, M_c, and A_ϕ into eq 6, along with the medium-dependent values of pH where appropriate (pH 2.2 buffer and pH 7.4 buffer), the effects of varying the copolymer composition on χ were examined. This analysis facilitated a quantitative study of the extent to which the magnitude of polymer−solvent interactions might be tuned by copolymerization techniques.

On the basis of measured values of the equilibrium polymer volume fractions, and using eq 6, χ values were calculated for each composition and each pH value. Table 10 gives the calculated χ values.

Theoretical values of χ were also calculated, using the following equation, developed by Hildebrand and Scatchard:[44]

$$\chi = 0.34 + \frac{V_1}{RT}(\delta_1 - \delta_2)^2 \quad (8)$$

Table 10. Calculated Values of Flory Polymer−Solvent Interaction Parameter χ and Binary Interaction Parameter l_{12} for Diacrylate Systems Having Various AA Contents and as a Function of pH

system	PEG/AA (mer/mer)	pH 2.2		pH 7.4	
		χ	l_{12}	χ	l_{12}
D2	1.0	1.94	−0.281	2.05	−0.273
D2−40	0.60	1.18	−0.311	0.38	−0.368
D3	1.5	1.74	−0.301	1.70	−0.304
D3−40	0.9	1.17	−0.320	0.64	−0.358
D4	2.0	1.45	−0.326	1.57	−0.317
D4−3	1.9	1.36	−0.331	1.43	−0.326
D4−10	1.8	1.32	−0.331	1.27	−0.335
D4−40	1.2	1.32	−0.315	0.81	−0.350
D9	4.5	0.99	−0.368	1.00	−0.367
D9−40	2.7	0.86	−0.363	0.56	−0.386

The parameter V_1 is the molar volume of the swelling agent; solubility parameters δ_1 and δ_2 were calculated by group contribution methods. The first term on the right-hand side of eq 8 is an entropic contribution, and the second term is an enthalpic contribution.

For the systems swollen in water, the measured χ values deviated strongly from the theoretical values. The deviations were observed due to the fact that the use of eq 8 to calculate the parameter χ is only valid for systems in which there are no specific polymer−solvent interactions, such as dipole interactions or hydrogen bonding. PEG and PAA are both known to participate in hydrogen bonding, and when such interactions between the polymer and the swelling agent are predominant, eq 8 must be generalized as follows:[45]

$$\chi = 0.34 + \frac{V_1}{RT}[(\delta_1 - \delta_2)^2 + 2l_{12}\delta_1\delta_2] \qquad (9)$$

The additional term on the right-hand side of eq 9 quantitatively accounts for the effects of specific interactions using l_{12}, a binary interaction parameter. Thus, by comparing the measured and theoretical values of χ for each composition in Table 10, it was possible to calculate a series of l_{12} values, indicative of the magnitude of hydrogen-bonding interactions in the various water-swollen copolymers.

The calculated values for the parameter l_{12} are given in Table 10. The binary interaction parameter increased in magnitude as the PEG chain length was increased at any given AA content and as the AA content was increased at any given PEG chain length. These trends reflect the increased hydrogen-bonding affinity of longer PEG chains and of copolymer networks of high AA content. The data also reflect ionization effects at pH 7.4. Most importantly, Table 10 shows that the nature of thermodynamic interactions between the multiacrylate copolymer networks and a penetrant can be precisely controlled by manipulation of the compositional parameters.

Conclusions

The composition-dependent structure and properties of model multiacrylate networks were explored. The measured glass transition temperatures were shown to reflect substantial free volume effects, which depended strongly on the compositional parameters of each system. The mechanical behavior of the networks indicated contributions due to PEG−PEG interactions. The strength of these interactions depended strongly on the AA content. The compositional dependence of the network structure was further explored by examining the equilibrium swelling behavior. These experiments indicated that manipulation of the compositional parameters offered a means of precisely tailoring the strength of polymer−solvent interactions.

Acknowledgment. This work was supported by grants from the National Science Foundation and the National Institutes of Health.

References and Notes

(1) Gossink, R. G. *Angew. Makromol. Chem.* **1986**, *145/146*, 365−389.
(2) Kloosterboer, J. G. *Adv. Polym. Sci.* **1988**, *84*, 1−61.
(3) Kloosterboer, J. G.; Lijten, G. F. C. M.; Boots, H. M. J. *Makromol. Chem., Macromol. Symp.* **1989**, *24*, 223−230.
(4) Kloosterboer, J. G.; van de Hei, G. M. M.; Gossink, R. G.; Dortant, G. C. M. *Polym. Commun.* **1984**, *25*, 322−325.
(5) Kloosterboer, J. G.; van de Hei, G. M. M.; Boots, H. M. J. *Polym. Commun.* **1984**, *25*, 354−357.
(6) Kloosterboer, J. G.; Lijten, G. F. C. M. *Polymer* **1987**, *28*, 1149−1155.
(7) Kloosterboer, J. G.; Lijten, G. F. C. M.; Zegers, C. P. G. *Polym. Mater. Sci. Eng.* **1989**, *60*, 122−126.
(8) Kloosterboer, J. G.; Lijten, G. F. C. M. *Polymer* **1990**, *31*, 95−101.
(9) Bowman, C. N.; Carver, A. L.; Kennett, S. N.; Williams, M. M.; Peppas, N. A. *Polymer* **1990**, *31*, 135−139.
(10) Bowman, C. N.; Peppas, N. A. *J. Appl. Polym. Sci.* **1991**, *42*, 2013−2018.
(11) Bowman, C. N.; Peppas, N. A. *Macromolecules* **1991**, *24*, 1914−1920.
(12) Kurdikar, D. L.; Peppas, N. A. *Polymer* **1994,** *35*, 1004−1011.
(13) Anseth, K. S.; Bowman, C. N.; Peppas, N. A. *Polym. Bull.* **1993**, *31*, 229−233.
(14) Anseth, K. S.; Bowman, C. N.; Peppas, N. A. *J. Polym. Sci., Polym. Chem.* **1994**, *32*, 139−147.
(15) Kurdikar, D. L.; Peppas, N. A. *Polymer* **1995**, *36*, 2249−2255.
(16) Anseth, K. S.; Wang, C. M.; Bowman, C. N. *Polymer* **1994**, *35*, 3243−3250.
(17) Anseth, K. S.; Wang, C. M.; Bowman, C. N. *Macromolecules* **1994**, *27*, 650−655.
(18) Anseth, K. S.; Kline, L. M.; Walker, T. A.; Anderson, K. J.; Bowman, C. N. *Macromolecules* **1995**, *28*, 2491−2499.
(19) Bland, M. H.; Peppas, N. A. *Biomaterials* **1996**, *17*, 1109−1114.
(20) Dietz, J. E.; Peppas, N. A. *Polymer* **1997**, *38*, 3767−3781.
(21) Moore, J. E. In *Chemistry and Properties of Crosslinked Polymers*; Labana, S. S., Ed.; Academic Press: New York, 1977; pp 535−546.
(22) Tyson, G. R.; Shultz, A. R. *J. Polym. Sci., Polym. Phys. Ed.* **1979**, *17*, 2059−2075.
(23) Hubca, G. H.; Oprescu, C. R.; Drăgan, G. H.; Dimonie, M. *Rev. Roumaine Chim.* **1982**, *27*, 433−442.
(24) Drăgan, G. H.; Hubca, G. H.; Oprescu, C. R.; Dimonie, M. *Rev. Roumaine Chim.* **1982**, *27*, 585−590.
(25) Miyazaki, K.; Takashi, H. *J. Biomed. Mater. Res.* **1988**, *22*, 1011−1022.
(26) Simon, G. P.; Allen, P. E. M.; Williams, D. R. G. *Polymer* **1991**, *32*, 2577−2587.
(27) Thakur, A.; Banthia, A. K.; Maiti, B. R. *J. Appl. Polym. Sci.* **1995**, *58*, 959−966.
(28) Tobita, H.; Hamielec, A. E. *Makromol. Chem. Macromol. Symp.* **1988**, *20/21*, 501−543.
(29) Tobita, H.; Hamielec, A. E. *Macromolecules* **1988**, *22*, 3098−3105.
(30) Kurdikar, D. L.; Peppas, N. A. *Macromolecules* **1994**, *27*, 4084−4092.
(31) Bowman, C. N.; Peppas, N. A. *J. Polym. Sci., Polym. Chem.* **1991**, *29*, 1575−1583.
(32) Bowman, C. N.; Peppas, N. A. *Chem. Eng. Sci.* **1992**, *47*, 1411−1419.
(33) Kurdikar, D. L.; Somvarsky, J.; Dusek, K.; Peppas, N. A. *Macromolecules* **1995**, *28*, 5910−5920.
(34) Anseth, K. S.; Rothenberg, M. D.; Bowman, C. N. *Macromolecules* **1994**, *27*, 2890.

(35) Odian, G. *Principles of Polymerization*, 3rd ed.; Wiley: New York, 1991; pp 452−531.
(36) Greenley, R. Z. In *Polymer Handbook*, 3rd ed.; Brandrup, J., Immergut, E. H., Eds.; Wiley: New York, 1989; pp II/267−II/274.
(37) Fox, T. G.; Loshaek, S. *J. Polym. Sci.* **1955**, *15*, 371.
(38) Grulke, E. A. *Polymer Process Engineering*; TPS Publishing: Lexington, KY, 1994; p 239.
(39) Van Krevelen, D. W. *Properties of Polymers: Correlations with Chemical Structure*; Elsevier: Amsterdam, 1972; pp 135−146.
(40) Flory, P. J.; Rehner, R. *J. Chem. Phys.* **1943**, *11*, 521.
(41) Peppas, N. A.; Lucht, L. M. *Chem. Eng. Commun.* **1984**, *30*, 291−310.
(42) Barar, D. G.; Staller, K. P.; Peppas, N. A. *J. Polym. Sci., Polym. Chem.* **1983**, *21*, 1013−1024.
(43) Barr-Howell. B. D.; Peppas, N. A. *Polym. Bull.* **1985**, *13*, 91−96.
(44) Gardon, J. L.; Teas, J. P. In *Treatise on Coatings*; Myers, R. R., Long, J. S., Eds.; Dekker: New York, 1976; Vol. 2, pp 413−476.
(45) Mikos, A. G.; Peppas, N. A. *Biomaterials* **1988**, *9*, 419−423.

MA980612S